

# 镁-裸钢板异种金属冷金属过渡熔钎焊连接机理

朱海霞<sup>1</sup>, 曹睿<sup>1</sup>, 李雅范<sup>2</sup>, 林巧力<sup>1</sup>, 陈剑虹<sup>1</sup>

(1. 兰州理工大学 有色金属先进加工与再利用省部共建国家重点实验室, 兰州 730050;

2. 哈尔滨电气动力装备有限公司, 哈尔滨 150000)

**摘 要:** 以 AZ61 镁合金焊丝为填充材料, 对 AZ31B 镁合金/Q235 裸钢板进行冷金属过渡熔钎焊试验研究, 分析不同工艺参数对焊缝成形和力学性能的影响. 并通过分析焊接接头微观组织及其元素分布状况来研究其连接机理. 研究表明: 随着送丝速度的增加, 接头最大抗拉载荷先升高后降低, 当焊缝宽度较大时, 断裂易发生在镁的热影响区, 其最大抗拉载荷可达 6 kN 以上; 焊缝及镁合金中的 Al 原子通过焊接过程扩散到界面上形成很薄的 Fe-Al 相反应层, 从而实现了镁-裸钢板的有效连接.

**关键词:** 冷金属过渡焊; 镁/裸钢板; 接头强度

**中图分类号:** TG 456.9 **文献标识码:** A **文章编号:** 0253-360X(2016)05-0077-04

## 0 序 言

镁合金作为最轻的结构金属材料以其具有独特的性能如比强度高、能量衰减系数大等<sup>[1]</sup>优点, 使得其在汽车工业上的应用优势远远超过其它材料. 目前, 汽车工业轻量化<sup>[1]</sup>已成为主流的发展方向, 如能实现镁/钢有效的连接, 不但可以更好的发挥镁合金在工业中的应用潜力而且可促进汽车、轨道客车等交通装备轻量化并节约能源.

镁和钢之间的物理性能差异很大, 同时镁、钢相互之间的固溶度极低, 不发生化学反应. 目前, 关于镁/钢焊接研究如激光焊<sup>[2]</sup>、搅拌摩擦焊<sup>[3]</sup>、扩散焊<sup>[4]</sup>等, 主要以添加中间层为主, 让其中间层和镁、钢发生化学反应以实现连接, 但衍生的另一问题是熔化钎料发生反应后生成的金属间化合物与钢基体物理性能差异大, 容易剥离, 造成界面结合强度的降低. 此外, 镁合金焊丝还会因镁蒸发、合金元素烧损等问题带来缩孔、过烧等缺陷, 造成表面成形不良.

因此有必要通过采用合适可控的热输入来获得较好的焊缝成形, 并保证界面充分结合. 文中采用冷金属过渡(CMT)焊接技术对 AZ31B 镁与 Q235 裸钢板进行搭接焊研究, 从焊缝形貌、微观组织及其力学性能几方面进行分析, 为镁和裸钢的连接提供一定的理论基础.

## 1 试验方法

### 1.1 试验材料

试验所采用的材料为 AZ31B 镁合金以及 Q235 裸钢板, 焊件尺寸为 100 mm × 200 mm × 1 mm; 焊丝型号为 AZ61 镁焊丝, 直径为 1.2 mm.

### 1.2 试验装置及方法

采用 Fronius 公司生产的 TPS3200 系列数字化 CMT 焊机对镁合金和裸钢板进行搭接焊. 焊前先用钢丝刷将裸钢板和镁合金试件表面的氧化膜去除, 再用丙酮和酒精去除镁合金和裸钢板上的油污和水渍. 将表面处理干净的试样组合成搭接接头(裸钢板在下, 镁合金在上), 采用高纯氩气作为保护气体, 冷金属过渡(CMT)一元线性系统进行焊接. 焊接装置如图 1 所示. 试验所用的焊接工艺参数如表 1 所示.

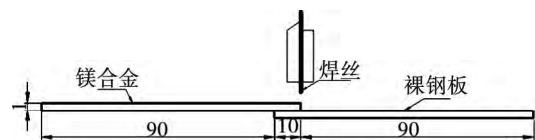


图 1 焊接装置图(mm)

Fig. 1 Schematic diagram of welding device

采用 Y-500 型 X 射线衍射仪、JSM-6700F 型扫描电镜(SEM)、能谱分析(EDAX)以及 CSS-2205 型电子万能拉伸试验机分别对接头的微观组织以及力学性能进行测试分析. 对于焊接接头力学性能的分析, 参照 GB/T2651-1989《焊接接头拉伸试验方法》

收稿日期: 2014-07-12

基金项目: 973 计划前期研究专项(2014CB660810), 国家自然科学基金资助项目(51265028)

用线切割机切成标准拉剪试样,如图2所示。

表1 焊接工艺参数  
Table 1 Welding parameters

序号	送丝速度 $v_f/(m \cdot \min^{-1})$	焊接速度 $v/(mm \cdot s^{-1})$	电压 $U/V$	电流 $I/A$	载荷 $F/kN$
1	6.0	5	8.4	68	2.60
2	6.5	5	8.7	75	4.54
3	7.0	5	9.4	84	5.05
4	7.5	5	10.0	85	5.32
5	8.0	5	10.3	102	5.55
6	8.5	5	10.4	104	5.68
7	9.0	5	10.5	108	5.96
8	9.5	5	10.3	117	6.23
9	10.0	5	11.9	130	6.44
10	10.5	5	12.5	136	4.80

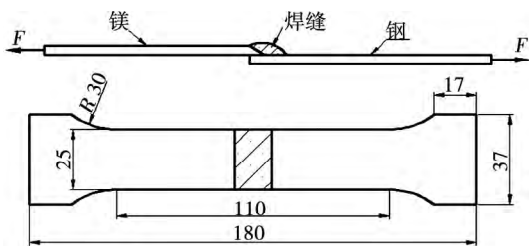


图2 焊接接头拉伸试样尺寸(mm)

Fig. 2 Schematic diagram of welding tensile (mm)

## 2 结果及分析

### 2.1 焊缝成形

图3所示为表1中9号接头的焊缝表面成形,该参数下所得焊接接头力学性能最好。观察焊缝可知,焊缝成形美观,接头表面连续均匀。

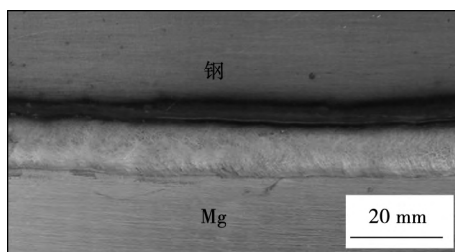


图3 焊缝表面成形

Fig. 3 Weld appearance

如图4所示,随着送丝速度的增加,焊缝宽度即结合界面的宽度均呈先增大而后略减小的趋势,而润湿角则呈先减小而后保持稳定的趋势且都大于 $90^\circ$ ,这从侧面说明镁合金焊丝在裸钢板上并没有良

好的润湿。结合上述形貌分析可知,随着送丝速度增加,焊接时热输入和填充的金属量增大,母材温度随之提高,焊缝填充金属润湿铺展能力也逐渐增加;当送丝速度增至 $10.5 m/\min$ 时,焊接过程就会失稳,出现大量飞溅并且镁板烧损严重,这使得焊缝宽度减少,反而不利于钎料的润湿铺展。

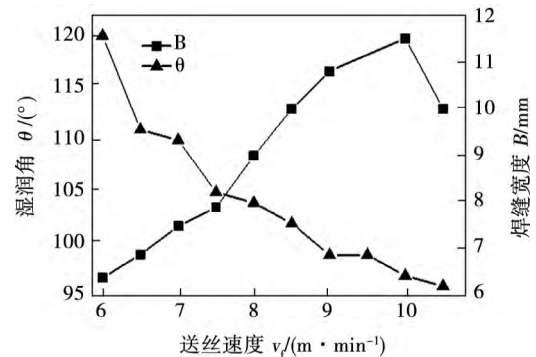


图4 润湿铺展能力与送丝速度的关系

Fig. 4 Relationship between wetting-spreading ability and wire feed speed

### 2.2 焊接接头的力学性能分析

将切好的标准拉伸试样在常温下进行拉伸试验。拉伸试验结果如表1所示。图5为焊接接头的平均最大抗拉载荷随送丝速度的变化图。

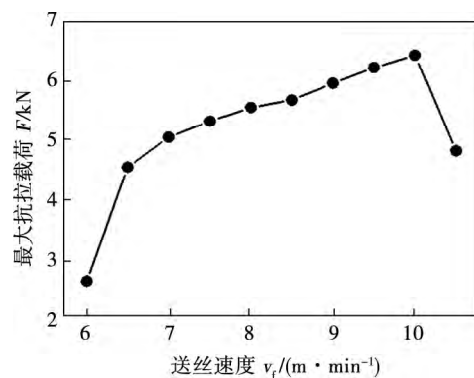


图5 焊接接头的最大抗拉载荷图

Fig. 5 Maximum tensile load of welded joints

结合表1及图5易知,随着送丝速度的增大,焊接电压及电流也逐渐增大,但焊接接头的平均最大抗拉载荷先增大后减小。这种变化趋势与图4中焊缝宽度的规律一致。容易推断,较大的焊缝宽度会造成结合界面的面积更大,则意味着在承载时受力面积更大,使接头发生塑性变形和最终断裂所需载荷更大。当焊接参数为表1中9号时,所得焊接接头的力学性能最好,接头所能承受的平均载荷为

6.44 kN 远远超过相同尺寸的镁-镀锌钢板搭接接头的强度<sup>[5]</sup>。

### 2.3 界面的微观组织

图 6 为表 1 中 9 号焊接接头的横截面。焊接接头由焊缝金属、结合区和熔合区三部分组成。焊接接头力学性能主要由熔合区和结合区决定。以下对这两个区域做详细的分析。

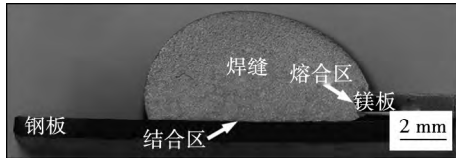


图 6 镁和裸钢板 CMT 熔钎焊接头特征

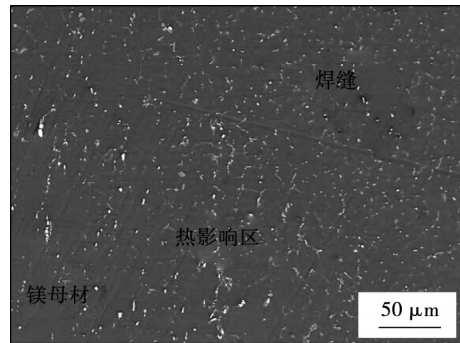
Fig. 6 Features of CMT welding-braze joint between magnesium and bare steel

图 7a 是熔合区的微观组织形貌, 焊接时镁合金一侧的部分母材熔化, 并与熔融的镁焊丝混合后形成熔焊接头。经能谱分析, 其中白色骨架状物质为镁铝金属间化合物  $Mg_{17}Al_{12}$ 。在靠近镁母材的热影响区由于经过高温加热, 晶粒会较母材变得粗大且各部分不均匀, 晶粒的不均匀性会造成塑韧性的不均匀, 在承载过程中易产生变形的不一致, 更容易产生微裂纹从而恶化接头的力学性能。因而可以得知在承载过程中镁合金的热影响区容易成为薄弱位置。

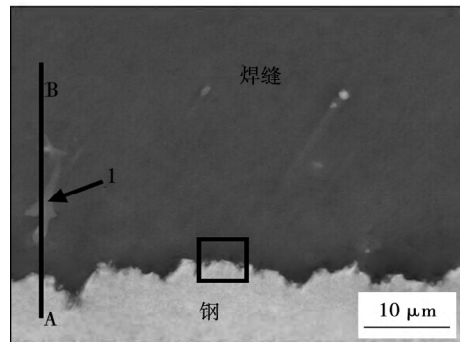
图 7b, c 为裸钢板/镁 CMT 焊接过程中结合界面的微观组织形貌, 由图可见, 裸钢板只有微熔, 结合界面通过焊缝金属与钢母材间原子的相互扩散最终在 Q235 裸钢板表面形成一层约  $0.8 \mu m$  反应层。反应层的存在证明了界面发生冶金结合, 产生了有别于母材的新相, 为了确定该相成分, 对界面做了 EDS 能谱分析, 结果如表 2 所示。根据表中对点 1 的测试结果可知, 焊缝中的骨架状物质是  $Mg_{17}Al_{12}$ 。由点 2 的能谱分析结果以及如图 8 所示结合面的 XRD 分析可以判断界面处除了  $\alpha-Mg$  的固溶体和  $\alpha-Fe$  的固溶体之外界面反应层主要包括  $FeAl$  金属间化合物。

为进一步分析钎焊界面处的原子分布情况, 对界面沿着线 AB 做线扫描能谱分析, 结果如图 9 所

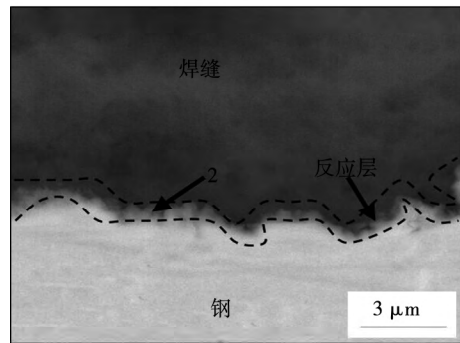
示。从图 9 可见在界面处 Al 元素发生了偏聚富集。这主要是由于 Fe 元素和 Al 元素之间的亲和能力较大, 从而在界面附近液态钎料中的 Al 原子在凝固的



(a) 熔合区



(b) 结合区



(c) 结合区放大

图 7 接头微观组织形貌

Fig. 7 Microstructure morphology of joint

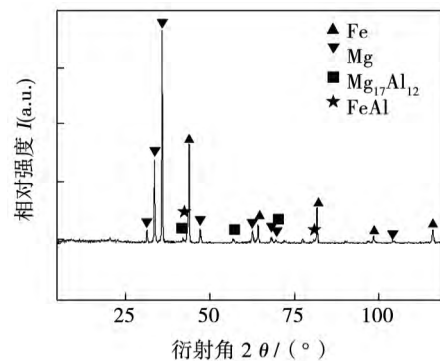


图 8 结合面的 XRD 分析结果

Fig. 8 XRD analysis at brazed interfaces

表 2 图 7 中 EDS 点成分分析(原子分数, %)

Table 2 EDS results of zones 1-2 in Fig. 7

测试点	Fe	Al	Mg
1	0	28.7	71.3
2	30.8	30.4	38.8

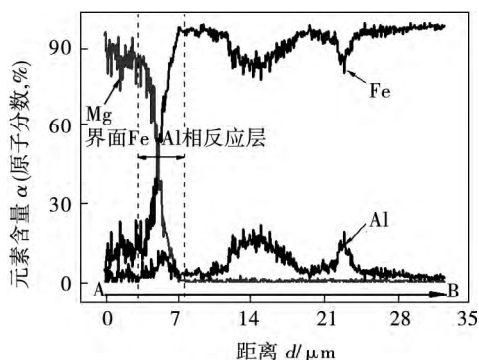


图9 界面的线能谱分析结果

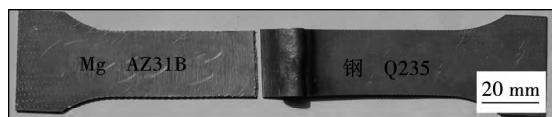
Fig. 9 Results of EDS line scanning at interface

过程中不断向含有铁溶质的界面附近聚集,造成了Al元素在界面的偏聚,从而在界面处形成Fe-Al相。

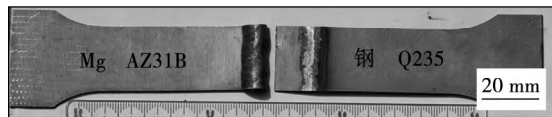
综上所述,镁和钢之间发生了冶金结合,产生了薄而均匀的界面层,这使得镁与裸钢润湿性虽不好但结合强度较高。

#### 2.4 焊接接头断裂

对于镁/裸钢板异种合金CMT熔钎焊接头进行拉伸试验,其断裂方式主要有两种,其中一种如表1中3~9号试样主要断裂在镁的热影响区,如图10a所示;另外一种如表1中1号2号试样则主要断裂在结合界面处,如图10b所示。



(a) 断裂在镁的热影响区



(b) 断裂在钎焊界面处

图10 不同接头的断裂方式

Fig. 10 Fracture modes of different joints

通过一系列拉伸试验所获得的接头最大抗拉载荷可知送丝速度较小(小于7 m/min)时,结合界面面积较小,焊接接头大多断裂在结合界面处;而当送丝速度合适(7 m/min~10 m/min)时,结合界面面积较大,接头则大部分断裂在镁的热影响区,因而当焊接参数合适,焊接接头最大抗拉载荷较高时,镁热影响区容易成为镁/裸钢板焊接接头的薄弱环节。

### 3 结 论

(1) 采用冷金属过渡技术(CMT)焊接方法能够实现镁/裸钢异种金属的有效连接,焊缝连续,成形较好。

(2) 通过微观组织分析发现,镁/裸钢板焊接接头的熔合区和焊缝主要由镁的固溶体 $\alpha$ -Mg以及骨架状的镁铝金属间化合物 $Mg_{17}Al_{12}$ 组成。结合界面主要靠铁和铝的金属间化合物FeAl连接。

(3) 镁/裸钢焊接接头润湿性虽不好,但因其界面处发生冶金反应,生成了新相,使得强度增高。且随着送丝速度的增加接头最大抗拉载荷和焊缝宽度都是先升高后降低,说明强度和结合界面有关。

(4) 当选择合适的焊接参数,焊接接头最大抗拉载荷较高时,镁/裸钢板焊接接头易断裂在镁母材的热影响区。

#### 参考文献:

- [1] 陈 军. 镁合金在汽车工业中应用与分析[J]. 材料研究与应用, 2010, 4(6): 81-84.  
Chen Jun. Application analysis of magnesium alloy in automotive industry[J]. Materials Research and Application, 2010, 4(6): 81-84.
- [2] 苗玉刚, 韩端峰, 姚竞争. 镁/钢异种金属激光深熔钎焊工艺特性[J]. 焊接学报, 2011, 32(1): 45-48.  
Miao Yugang, Han Duanfeng, Yao Jingzheng. Welding characteristic of laser welding-brazed Mg/steel dissimilar alloys[J]. Transactions of the China Welding Institution, 2011, 32(1): 45-48.
- [3] 黄勇兵, 李建萍, 黄春平, 等. 镁和钢搅拌摩擦焊接头组织分析[J]. 焊接学报, 2013, 34(5): 67-70.  
Huang Yongbing, Li Jianping, Huang Chunping, et al. Microstructure of friction stir welded joint of magnesium and steel[J]. Transactions of the China Welding Institution, 2013, 34(5): 67-70.
- [4] Pierre D, Viala J C, Peronnet M, et al. Interface reactions between mild steel and liquid Mg-Mn alloys[J]. Material Science and Engineer A, 2003, 34(9): 256-264.
- [5] 曹 睿, 余建永, 陈剑虹, 等. 镁/镀锌钢板CMT熔钎焊连接机制分析[J]. 焊接学报, 2013, 34(9): 21-24.  
Cao Rui, Yu Jianyong, Chen Jianhong, et al. Bonding mechanism of CMT fusion-brazed joints between magnesium and galvanized steel[J]. Transactions of the China Welding Institution, 2013, 34(9): 21-24.

作者简介: 朱海霞,女,1993年出生,硕士研究生。主要从事异种金属的焊接性研究,发表论文3篇。Email: 1060870005@qq.com

通讯作者: 曹 睿,女,博士,教授,博士研究生导师。Email: caorui@lut.cn

hanced by increasing the area of real intimate contact. The paper presented electron beam texturing on Kovar alloy to improve the surface micro-roughness. The wetting behavior of borosilicate glass on textured Kovar alloy was investigated by sessile drop method. The results indicated that the increase of effective contact area by using electron beam texturing facilitated the spreading of molten glass. The contact angle decreases continuously with the increase of heating temperature and holding time. The main reaction products between glass and oxide layer are  $\text{Fe}_2\text{SiO}_4$ . The high-energy beam texturing and pre-oxidation on the metal surface promoted the mechanical-chemical bonding of glass and metal effectively, which improves the connection strength of glass and metal.

**Key words:** borosilicate glass; Kovar alloy; wetting behavior; electron beam texturing; mechanical-chemical bonding

#### Temperature uniformity control on specimen of material testing apparatus in hydrogen environment

LIU Xiaoliang<sup>1,2</sup>, CHEN Xuedong<sup>1,2</sup>, WANG Bing<sup>1,2</sup>, FAN Zhichao<sup>1,2</sup>, ZHUANG Qingwei<sup>3</sup>, FAN Hui<sup>3</sup>, CHI Chengfang<sup>3</sup> (1. Hefei General Machinery Research Institute, Hefei 230031, China; 2. National Safety Engineering Technology Research Center for Pressure Vessels and Pipeline, Hefei 230031, China; 3. Changchun Research Institute for Mechanical Science Co. Ltd., Changchun 130012, China). pp 65-68

**Abstract:** A new testing apparatus in hydrogen environment was developed for studying the degradation of material properties by hydrogen which is the most common type of damages induced by gas. The temperature uniformity of specimen is the key to ensure the creditability and accuracy of the testing results. Another water-cooling structure was added on the top of the pressure vessel to take away the excessive thermal gathered at the upper specimen. A new fuzzy-PID control algorithm was proposed to enhance the accuracy of temperature uniformity. The fuzzy algorithm is used to set the power upper limit of both upper and lower resistive heater respectively, and then the traditional PID algorithm is used to control the power of each resistive heater separately. The experiment results indicate that the new heater structure and fuzzy-PID control algorithm improved the temperature uniformity of the specimen, and the temperature difference between upper and lower of the specimen was control within  $\pm 1^\circ\text{C}$ , which meet the demands of material performance testing.

**Key words:** specimen; temperature uniformity; fuzzy control; hydrogen damage; testing apparatus

#### Study on fusion welding of magnesium alloy to steel by hybrid laser-TIG welding with interlayer

SONG Gang, WANG Jie, YU Jingwei, LIU Liming (Key Laboratory of Liaoning Advanced Welding and Joining Technology, School of Materials Science and Engineering, Dalian University of Technology, Dalian 116024, China). pp 69-72

**Abstract:** Compared with single heat source, laser-TIG hybrid welding with the characteristic of optimum-designed heat source energy density and thermal-mechanical coupling mode is put to achieve precise forming and excellent properties in high-end equipment welding. This paper focuses on realizing high quality fusion welding of magnesium alloy to steel with Cu-Zn interlayer by utilizing the gradient energy density characteristic of laser-TIG heat source. The new idea of multicomponent liquid phase coexistence is put forward in welding magnesium to steel by hybrid laser-TIG welding, meanwhile the effect of Al element is analysed in the welding.

**Key words:** hybrid Laser-TIG; dissimilar metals; multicomponent liquid phase; fusion welding

#### Failure mode and mechanism of BGA lead-free solder joints under drop-impact load

WEN Guichen<sup>1</sup>, LEI Yongping<sup>1</sup>, LIN Jian<sup>1</sup>, GU Jian<sup>1</sup>, BAI Hailong<sup>2</sup>, QIN Junhu<sup>2</sup> (1. Beijing University of Technology, Beijing 100124, China; 2. Yunnan Tin Material Co., Ltd., Kunming 650217, China). pp 73-76

**Abstract:** The failure mode and mechanism of BGA packages were explored by drop tests of PCB packages. Furthermore, the initiation mechanism and expanding features of cracks were analyzed in this work. Results showed that, cracks in the solder joints and structural fractures of PCB are the main reasons that cause the failure of BGA packages. There are two main kinds of cracks in solder joints which distribute on the joint top and bottom, and the initiation mechanism of them are different. Micro gaps between the solder joint and solder resist film that caused by gravity contribute to the cracks on the top. Cracks on the bottom are caused by the gaps on both sides of the remained solder flux that existed between the solder joint and the solder resist film under drop-impact load. The expanding of cracks has a relationship with the original location, orientation and stress conditions of the crack sources. Relative position of solder joint and pad also have important influence on the expanding of cracks.

**Key words:** BGA; lead-free solder joints; drop-impact; failure mode; failure mechanism

#### Joining mechanisms of cold metal transfer welding-brazing of Mg to bare steel

ZHU Haixia<sup>1</sup>, CAO Rui<sup>1</sup>, LI Yafan<sup>2</sup>, LIN Qiaoli<sup>1</sup>, CHEN Jianhong<sup>1</sup> (1. State Key Laboratory of Advanced Processing and Recycling of Non-ferrous Metals, Lanzhou University of Technology, Lanzhou 730050, China; 2. Harbin Electric Power Equipment Co., Ltd, Harbin 150000, China). pp 77-80

**Abstract:** AZ31B magnesium alloys and Q235 bare steel are joined by cold metal transfer process with AZ61 Mg based filler wire. The effects of processing parameters on weld appearance and mechanical properties are studied. The joining mechanism is studied by analyzing the microstructure and distribution of elements of welded joints. The results indicate that the tensile strength of the joints first increased and then decreased with the increase of the wire feed speed. The joint with larger weld width is fractured in the magnesium heat affected zone and has a tensile load more than 6 kN. Mg and bare steel can be efficiently joined by the thin interfacial reaction layers with Fe-Al phase, which is attributed to the diffusion of the element Al.

**Key words:** cold metal transfer; Mg/bare steel; joint strength

#### Fatigue analysis of TC11/TC17 heterogeneous titanium alloy linear friction jointing

WANG Hongfeng, WANG Jianli, ZUO Dunwen, SONG Weiwei, JI Ling (1. College of Mechanical and Electrical Engineering, Huangshan University, Huangshan 245041, China; 2. College of Mechanical and Electrical Engineering, Nanjing University of Aeronautics and Astronautics, Nanjing 210016, China). pp 81-84

**Abstract:** Two heterogeneous titanium alloy TC11 and TC17 was jointed by linear friction jointing. The relationship between load and displacement and the relationship between temperature and the fatigue cycle time with increasing temperature under the cyclic loading were analyzed by the fatigue testing machine. The results show that the relationship between load and displacement curve was leaf, and with the increasing of cycle time, leaf width became narrow gradually, finally turned into a straight line. But when the heating temperature increased to more than 1/3 of the titanium alloy melting point, the relationship between load and displacement curve will occur distortion. Temper-